Available online at www.sciencedirect.com

ScienceDirect

Procedia Engineering 81 (2014) 2036 – 2041

Procedia Engineering

www.elsevier.com/locate/procedia

11th International Conference on Technology of Plasticity, ICTP 2014, 19-24 October 2014, Nagoya Congress Center, Nagoya, Japan

Mechanical property of Al alloy joints by friction stir blind riveting

Junying Min[a], Jingjing Li[a], Blair E. Carlson[b], Yongqiang Li[b], Jianping Lin[c,*]

[a]*Department of Mechanical Engineering, University of Hawaii at Manoa, 2540 Dole Street Honolulu, HI 96822, USA*
[b]*General Motors Research & Development, Warren, MI 48095-9055, USA*
[c]*School of Mechanical Engineering, Tongji University, Shanghai 201804, China*

Abstract

Dissimilar lap-shear joints were fabricated by the friction stir blind riveting process using AA6111 (0.9 mm) as the top-sheet and AA6022 (2.0 mm) as the bottom-sheet in a 2-sheet stack-up. Tensile testing of the friction stir blind riveting joints exhibited a combined fracture mode of initial shear followed by tearing. The maximum tensile load of the friction stir blind riveting joints increases slightly with increasing feed rate and shows little dependence on the spindle speed. The microhardness of the material at different layers along with the rivet penetration are analyzed and discussed.

Selection and peer-review under responsibility of the Department of Materials Science and Engineering, Nagoya University

Keywords: Friction stir; Blind riveting; Al alloys

1. Introduction

Aluminum alloys have been widely applied to vehicles to realize mass savings which lead to fuel economy improvements and ultimately CO_2 emission reductions. However, the joining of Al alloy sheets with similar and dissimilar materials continues to be an issue. Numerous innovative joining technologies have been developed to join similar and dissimilar sheet metals (Cao et al., 2006; Mori et al., 2013; Casalino et al., 2013; Silva et al., 2013). An example of this is friction stir welding, which was invented by The Welding Institute (Thomas et a., 1991) and is a solid state welding process. This process has the advantage that it can avoid the problems of solidification

* Corresponding author. Tel.: +8613901719457
E-mail address: jplin58@tongji.edu.cn

Selection and peer-review under responsibility of the Department of Materials Science and Engineering, Nagoya University
doi:10.1016/j.proeng.2014.10.277

cracking and porosity associated with conventional fusion welding processes and because of this increase the joint efficiency relative to fusion welding methods (Xu et al., 2009). A number of related variants, e.g. friction stir spot welding (Yuan et al., 2011), friction drilling (Miller et al., 2006) etc., have been developed by scholars in recent years.

Very recently, a friction stir blind riveting process has been proposed by (Wang and Stevenson, 2007; Gao et al., 2007). This process is a combination of the friction stir process and the blind riveting process and eliminates the need for predrilling as in the conventional blind riveting process. In friction stir blind riveting, a blind rivet is held by a spindle and engages the workpieces at a high spindle speed. This high speed rotation of the rivet generates frictional heat enabling the rivet to penetrate the workpieces until the rivet head engages the top workpiece. Because of the significant heat generated by the friction stirring, the penetration force can be kept to comparatively low levels. Once the head engages the top workpiece, the mandrel of the rivet is pulled using a rivet gun until it fractures at its notch resulting in both workpieces being locked tightly together, refer to Figure 1.

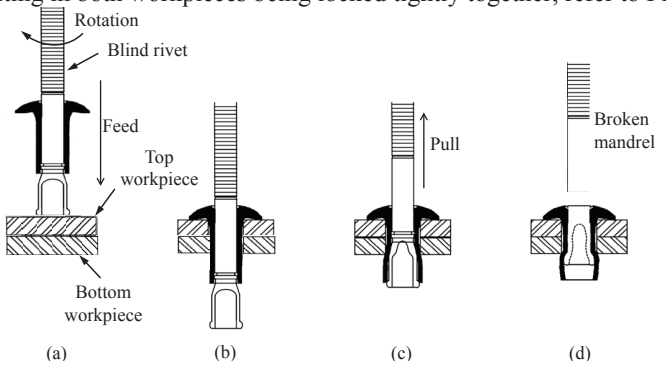

Fig. 1. Illustration of the friction stir blind riveting process. (a) The rotating blind rivet approaches the workpieces, (b) the blind rivet reaches its destination, (c) the mandrel is pulled by a rivet gun and (d) the mandrel breaks at its notch and a finished joint is fabricated.

It has been demonstrated that joints fabricated using similar and dissimilar materials such as Al alloys, Mg alloys and steel can be fabricated by this new joining process (Gao et al., 2007; Lathabai et al., 2011). Gao et al. (2007) completed friction stir blind riveting tests on AA5052 sheets with a thickness of 3 mm and found that the friction stir blind riveting joints clearly possessed greater tensile loads and better fatigue resistance than resistance spot welded joints. With the friction stir blind riveting process, both die cast and wrought Al alloys as well as Mg AZ31 were joined by Lathabai et al. (2011), where several types of blind rivets were tried.

In this work, joints of AA6111-T4 (0.9 mm) and AA6022-T4 (2.0 mm) were successfully fabricated using the friction stir blind riveting process at spindle speeds of 6000 and 9000 rpm and various feed rates. Tensile tests were carried out to obtain the mechanical properties of the joints.

2. Experimental details

Initial testing showed that the rivet in the AA6111-AA6111 friction stir blind riveting joint slips out from the bottom AA6111 workpiece during tensile testing, i.e. the rivet is not able to lock the thinner AA6111 workpiece (0.9 mm) when it is placed on the bottom, but it can lock the thicker AA6022 workpiece (2.0 mm) when it is used as the bottom sheet. Therefore, the thicker AA6022 workpiece was kept as the bottom sheet and the thinner AA6111 as the top sheet in all subsequent friction stir blind riveting tests discussed in this report.

2.1. Friction stir blind riveting tests

Lap-shear AA6111-AA6022 joints were fabricated by the friction stir blind riveting process, where the AA6111 and AA6022 workpieces were placed on the top and bottom, respectively, and the Avdel® SSPV-06-04 rivet with a shank diameter of 4.8 mm (see Fig. 2) was employed. The spindle speeds (ω) were set at 3000, 6000 and 9000

rpm, and the feed rates (f) were given as 120, 420 and 780 mm/min. However, the AA6111-AA6022 joints failed during friction stir blind riveting when ω = 3000 rpm, regardless of feed rate, and as such was excluded from subsequent testing. Consequently, testing was completed onAA6111-AA6022 joints fabricated under six combinations of spindle speeds and feed rates. After the frictional penetration was finished, the mandrel was pulled backward using a manual rivet gun to fasten the workpieces. Once the mandrel reached its predetermined break-load, the spent portion of the mandrel broke at the notch and was released from the set rivet.

To understand the microhardness evolution during friction stir blind riveting, two friction stir blind riveting tests were interrupted at rivet travel distances of 0.5 and 2.0 mm, namely, the penetration of mandrel tips were halted such that the maximum penetration was in the AA6111 and AA6022 workpieces, respectively. For the interrupted tests, the spindle speed was fixed at 6000 rpm and feed rate at 780 mm/min. The mandrel in the interrupted joints was not pulled.

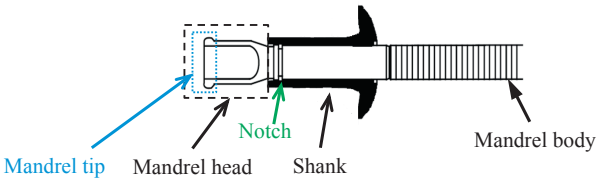

Fig. 2. Illustration of the Avdel® SSPV-06-04 rivet.

2.2. Tensile tests

The fully completed joints were pulled to fracture using an Instron 5582 tensile machine at a crosshead speed of 5 mm/min. Two spacers were used to keep the joint pulled along the tensile axis and thus prevent bending.

2.3. Microhardness measurements

The interrupted and full completed joints were sectioned and polished for microhardness measurements (HV0.3) using a LECO LM247AT microhardness tester. A pattern of microhardness indentations was applied as shown in Fig. 3. Note, the black diamond symbols indicate the locations where the indenter pressed. The microhardness was also measured through the thickness direction, where four layers were selected at an interval of 250 μm. The hardness baseline of each individual layer was chosen from the left dashed zone (away from the rivet) with 3 replicates, and compared to the hardness measured in the right dashed zone (zone possibly affected by friction stir blind riveting).

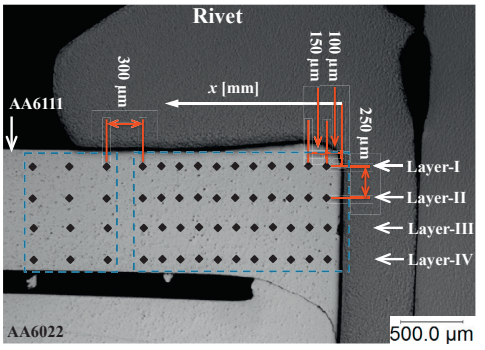

Fig. 3. Illustration of the pattern used for microhardness measurements on the sectioned and polished AA6111 workpiece of a friction stir blind riveting joint.

3. Results and discussion

3.1. Tensile testing results

Fig. 4a shows the load vs. displacement curves of the friction stir blind riveting joints formed under a range of process parameters. Figure 4b shows both the front and side views of a pulled and fractured friction stir blind riveting joint with a spindle speed of 6000 rpm and a feed rate of 780 mm/min. The thicker AA6022 workpiece which had nearly no bending deformation during tensile testing was locked by the rivet thus, the majority of the displacement was a result of the thinner AA6111 workpiece tearing. Therefore, the mechanical properties of the AA6111-AA6022 joints are mostly a function of the AA6111 workpiece properties, which is the weakest part in this joint. From the detailed view in Fig. 4c it is concluded that the AA6111 workpiece first sheared the sheet and then eventually tore the sheet until fracture. The tensile testing results show that this combined shearing + tearing fracture mode is common for all AA6111-AA6022 joints fabricated by either friction stir blind riveting or the conventional blind riveting process. In other words, the friction stir blind riveting process does not change the failure mode of the AA6111-AA6022 joints in tensile tests compared to conventional method.

In reference to Fig. 4a, the load vs. displacement curves can be divided into two parts: Part-I, which ends with the sharp drop on the load curve, is associated with the rivet/sheet shearing process, e.g. 0-5.9 mm region on the AA6111-AA6022 joint load curve. Note the joints were fabricated with a spindle speed of 6000 rpm and a feed rate of 120 mm/min. Part-II corresponds to the tearing process, e.g. the load curve beyond 5.9 mm displacement. Figure 4d is a plot of maximum tensile load versus feeding rate for the joints. It is shown that the maximum tensile load increases slightly with increasing feed rate, and there is very little dependence upon the spindle speed.

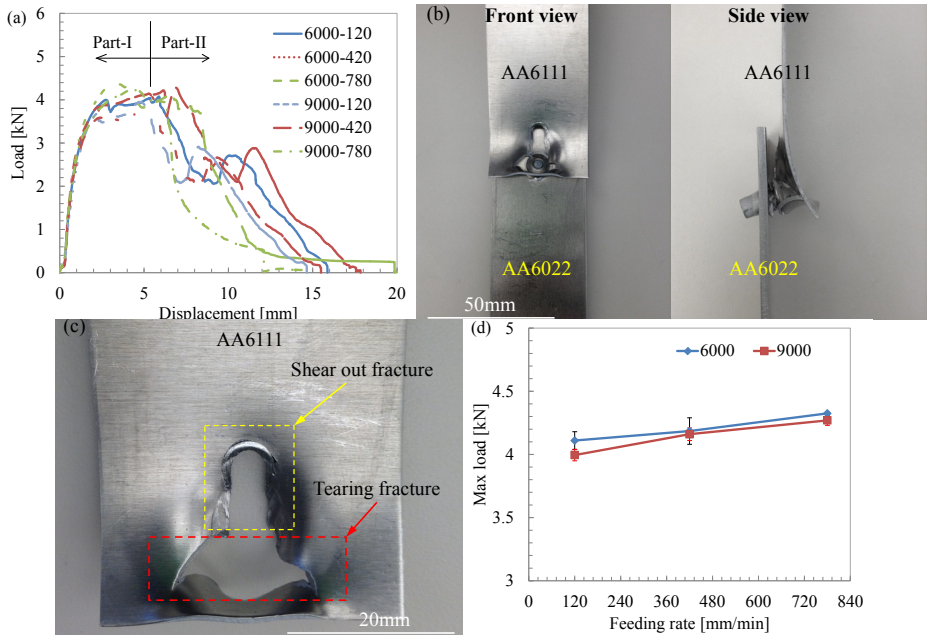

Fig. 4. (a) Load vs. displacement curves of friction stir blind riveting joints, (b) a fractured joint with a spindle speed of 6000 rpm and a feed rate of 780 mm/min, (c) detailed view showing the failure mode on the AA6111 workpiece and (d) the dependence of the maximum tensile load of the joints on the spindle speed and feeding rate.

3.2. Microhardness

As described in Section 2.3, the baseline microhardness ($HV0.3_{base}$) of each sheet was computed from the diamond shaped indents left in the polished surface in the left zone as shown in Fig. 3. The relative hardness (R_H)

on each layer was calculated as the ratio of the actual measured microhardness ($HV0.3$) and the baseline microhardness ($HV0.3_{\text{base}}$), namely,

$$R_H = HV0.3 / HV0.3_{base}. \quad (1)$$

Fig. 5 is a set of graphs which shows the relative hardness distribution of the AA6111 top-sheet material for both interrupted joints and a fully completed joint all fabricated under the process parameters of ω = 6000 rpm and f = 780 mm/min. In the interrupted joint with a mandrel penetration distance 0.5 mm, R_H differs from layer to layer as observed in Fig. 5a. R_H of each layer decreases when x (refer to Fig. 5) increases to a critical distance, x_c, and beyond x_c, R_H becomes a constant value of ~1, which indicates that the hardness was not affected by the frictional penetration process. x_c decreases from the upper layer to the lower layer, e.g. x_c = 0.85 mm for Layer-I and x_c = 0.25 mm for Layer-IV. Among these four layers, Layer-I that is closest to the top surface of the AA6111 workpiece, possesses the highest hardness in the range of $x < x_c$, which is due to the fact that the material close to the shank and near the top surface of the AA6111 workpiece underwent large amounts of deformation. In the interrupted joint for a mandrel penetration distance of 2.0 mm, i.e. the AA6111 top-sheet was fully penetrated, the variation between the hardness traverse layers was reduced and x_c increased to 1.15 mm as shown in Fig. 5b. The hardness decrease in Layer-I may be a result of greater heat input since the greater mandrel penetration distance equates to longer process time and greater overall heat input. In the fully completed joints (Fig. 5c), the hardness of Layers-I, II and III is lower compared to the interrupted joint in Fig. 5b. This could be attributed to a longer heat treatment period as mentioned above since the mandrel penetrated through both workpieces in the fully completed joint. However, when the rivet penetrated through the two workpieces (the case shown in Fig. 5c), the material close to the bottom surface of the AA6111 workpiece underwent additional deformation; hence, the hardness of Layer-IV increased and the hardness of other layers decreased compared to Fig. 5b. As a result, Layer-IV has the highest hardness among these four layers in the range of $x < x_c$.

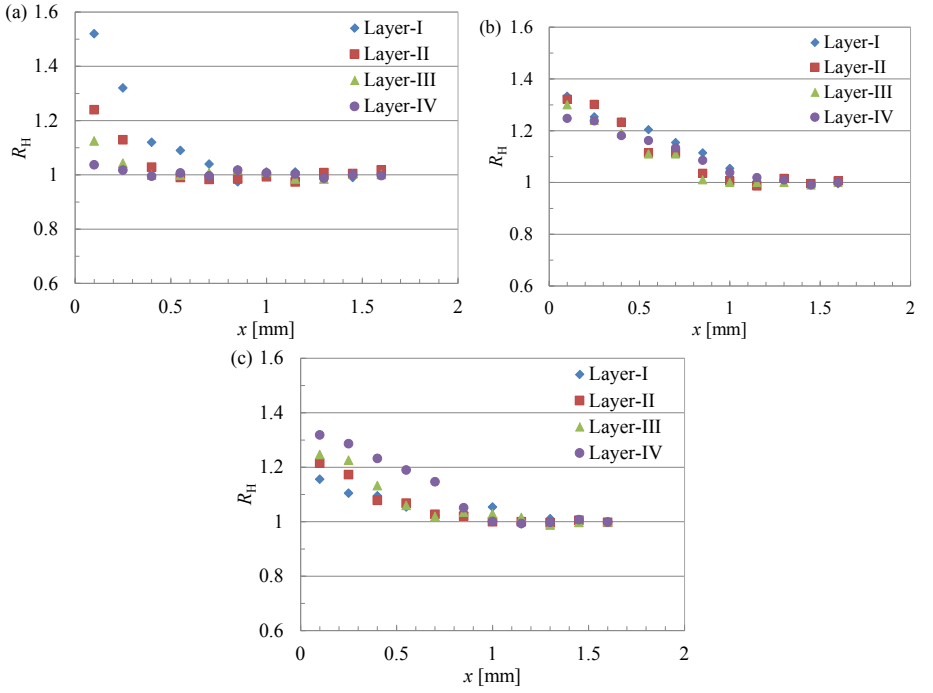

Fig. 5. Relative hardness (R_H) distribution of the AA6111 top-sheet in an interrupted joint along the x-axis, refer to Fig. 3, where x =0 is the interface between the shank and top sheet and positive x is distance in the top-sheet away from this interface. The relative hardness distribution graphs are for interrupted mandrel penetration distances of (a) 0.5 mm and (b) 2.0mm and the fully completed joint (c).

4. Summary remarks

AA6111 and AA6022 sheets were joined in a lap-shear configuration by the friction stir blind riveting process using a range of spindle speeds and feed rates. In the joints, the thinner AA6111 workpiece was defined as the top sheet. The tensile testing results show that fracture of the AA6111-AA6022 joints occurred in the AA6111 workpieces by the rivet first shearing the material followed by a tearing mode. The maximum tensile load of the joints increased slightly with feed rate and exhibited no statistical dependence upon spindle speed for the range of feed rates investigated.

The hardness of the AA6111 material within a distance of 1.15 mm to the shank is affected by the frictional penetration process of the rotating rivet, and the hardness decreases with increasing distance from the shank. This affected zone still needs to be further studied to distinguish different zones, e.g. heat affected zone, thermomechanical affected zone etc.

Acknowledgements

The authors would like to thank Anthony J. Blaszyk and Dr. John S. Agapiou for their help in the friction stir blind riveting tests. Financial support for this research was provided through the General Motors collaborative research at The University of Hawaii, USA and the project under grant No.51375346 of the National Natural Science Foundation of China. The authors wish to thank the GM Manufacturing Systems Research Laboratory for experimental and technical supports.

References

Cao, X., Jahazi, M., Immarigeon, J.P., Wallace, W., 2006. A review of laser welding techniques for magnesium alloys. Journal of Materials Processing Technology, 171, 188-204.

Mori, K., Abe, Y., Kato, T., 2013. Self-pierce riveting of multiple steel and aluminium alloy sheets. Journal of Materials Processing Technology, http://dx.doi.org/10.1016/j.jmatprotec.2013.09.007.

Casalino, G., Campanelli, S.L., Dal Maso, U., Ludovico, A.D., 2013. Arc Leading Versus Laser Leading in the Hybrid Welding of Aluminium Alloy Using a Fiber Laser. Procedia CIRP, 12, 151-156.

Da Silva, J., Costa, J.M., Loureiro, A., JFerreira, M., 2013. Fatigue behaviour of AA6082-T6 MIG welded butt joints improved by friction stir processing. Materials and Design, 51, 315-322.

Thomas, W.M., Nicholas, E.D., Needham, J.C., Church, M.G., Templesmith, P., Dawes, C.J., 1991. Friction stir welding. International Patent Application no. PCT/GB92102203 and Great Britain Patent 9125978.8.

Xu, W., Liu, J., Luan, G., Dong, C., 2009. Microstructure and mechanical properties of friction stir welded joints in 2219-T6 aluminum alloy. Materials and Design, 30, 3460-3467.

Yuan, W., Mishra, R.S., Webb, S., Chen, Y.L., Carlson, B., Herling, D.R., Grant, G.J., 2011. Effect of tool design and process parameters on properties of Al alloy 6016 friction stir spot welds. Journal of Materials Processing Technology. 211, 972-977.

Miller, S.F., Tao, J., Shih, A.J., 2007. Friction drilling of cast metals. International Journal of Machine Tools & Manufacture, 46, 1526-1535.

Wang, P.C., Stevenson, R., 2007. Friction stir rivet and method of joining, US Patent 7862271.

Gao, D., Ersoy, U., Stevenson, R., Wang, P.C., 2009. A new one-sided joining process for aluminum alloys: Friction Stir Blind Riveting, ASME Journal of Manufacturing Science and Engineering, 131, 061002-1-12.

Lathabai, S., Tyagi, V., Ritchie, D., Kearney, T., Finnin, B., 2011. Friction Stir Blind Riveting: A Novel Joining Porcess For Automotive Light Alloys. SAE2011-01-0477.